Skutterudites under pressure: An ab initio study

Swetarekha Ram, V. Kanchana, and M. C. Valsakumar

Skutterudites under pressure: An *ab initio* study

Swetarekha Ram,[1] V. Kanchana,[1,a)] and M. C. Valsakumar[2]

[1]*Department of Physics, Indian Institute of Technology Hyderabad, Ordnance Factory Estate, Yeddumailaram 502 205, Andhra Pradesh, India*
[2]*School of Engineering Sciences and Technology (SEST), University of Hyderabad, Prof. C. R. Rao Road, Gachibowli, Hyderabad 500 046, Andhra Pradesh, India*

Ab initio results on the band structure, density of states, and Fermi surface (FS) properties of $LaRu_4X_{12}$ (X = P, As, Sb) are presented at ambient pressure as well as under compression. The analysis of density of states reveals the major contribution at the Fermi level to be mainly from the Ru-*d* and X-*p* states. We have a complicated Fermi surface with both electron and hole characters for all the three compounds which is derived mainly from the Ru-*d* and X-*p* states. There is also a simpler FS with hole character derived from the P-p_z orbital for $LaRu_4P_{12}$ and Ru-d_{z^2} orbital in the case of As and Sb containing compounds. More interestingly, Fermi surface nesting feature is observed only in the case of the $LaRu_4P_{12}$. Under compression, we observe the topology of the complicated FS sheet of $LaRu_4As_{12}$ to change around $V/V_0 = 0.85$, leading to a behaviour similar to that of a multiband superconductor, and in addition, we have two more hole pockets centered around Γ at $V/V_0 = 0.8$ for the same compound. Apart from this, we find the hole pocket to vanish at $V/V_0 = 0.8$ in the case of $LaRu_4Sb_{12}$ and the opening of the complicated FS sheet gets reduced. The de Haas van Alphen calculation shows the number of extremal orbits in the complicated sheet to change in As and Sb containing compounds under compression, where we also observe the FS topology to change. © *2014 AIP Publishing LLC*. [http://dx.doi.org/10.1063/1.4867041]

I. INTRODUCTION

Rare-earth filled skutterudites with the general formula RT_4X_{12} have attracted much attention due to their various unique physical properties such as occurrence of a pressure-induced superconducting phase in $PrRu_4P_{12}$,[1] multiple ordered state in $SmRu_4P_{12}$,[2] magnetic field independent heavy fermion state in $SmOs_4P_{12}$,[3] metal-insulator transition in $PrFe_4P_{12}$[4] and in $SmRu_4P_{12}$,[2] heavy-fermion superconductivity in $PrOs_4Sb_{12}$,[5–7] and highly promising thermo-electric properties in some others.[8–10] The interesting point is that most of the above properties of these compounds are certainly linked with the Fermi surface (FS) topology. It is to be noticed that the metal-insulator transition occurring in $PrRu_4P_{12}$[11] is associated with FS nesting with $2\pi/a(1,0,0)$ as the nesting vector $\vec{q}$. Numerous studies have been performed to explain Fermi surface topology of isostructural $LaRu_4P_{12}$[11] and the authors have found FS nesting with $\vec{q} = 2\pi/a(1,0,0)$. From the above discussion, one can expect a similar metal-insulator transition in $LaRu_4P_{12}$. However, resistivity and specific-heat measurements show no such transition above the superconducting transition temperature (T_c).[12] Our present calculations on $LaRu_4P_{12}$ also exclude such type of transition which is consistent with the available reports. Apart from this, recently, experimental as well as theoretical calculation on superconductivity and the Vibrational properties of some As and P containing compounds of the form LaT_4X_{12} (T = Fe, Ru, Os; X = As, Sb) and LaT_4P_{12} (T = Fe, Ru) are reported.[13,14] From these experimental studies, it was found that the T_c decreases

under pressure in the case of $LaRu_4P_{12}$, and in our present calculation, we try to correlate and predict this decreasing behaviour of T_c under pressure from the electronic structure calculation.[14]

Fermi surface studies are also available for $LaOs_4Sb_{12}$[15] and $LaOs_4P_{12}$,[16] but the authors have not found any nesting feature in $LaOs_4Sb_{12}$. Experimentally de Haas van Alphen (dHvA) studies are available for $LaFe_4P_{12}$[17] and $LaRu_4P_{12}$[18] and $CeRu_4Sb_{12}$,[19] where the authors have found the FS topology of $CeRu_4Sb_{12}$ and $LaRu_4Sb_{12}$ to be different due to the presence of strong electron correlation in the former compound. One of the characteristic features of some of the filled skutterudites is multi-band superconductivity. Recently, Bochenek *et al.*[20] have reported multiple-gap superconducting behaviour in $LaRu_4As_{12}$ from the observed nonlinear magnetic-field dependence of the specific heat in the zero-temperature limit, a positive curvature of the upper critical field in the vicinity of T_c, and a deviation of the electronic specific heat from the one-gap model. The origin of multiband effect was reported in $PrRu_4As_{12}$[21,22] by comparing it with the iso-structural compound $LaRu_4As_{12}$. Apart from these, the position parameters *u* and *v* of the X atom also play a role in determining the electronic and various physical properties.[23] Recently, Uchiumi *et al.*[12] have reported the superconducting transition temperature of $LaRu_4X_{12}$ with X = P, As, Sb to be 7.2, 10.3, and 2.8 K, respectively. Among all the rare earth filled skutterudite compounds, $LaRu_4As_{12}$ is having the highest superconducting transition temperature of 10.3 K.[12,24] From the available literature on these skutterudites, it is quite evident that the FS topology studies on these compounds are mandatory and highly essential to have a complete understanding of the

a)Author to whom correspondence should be addressed. Electronic mail: kanchana@iith.ac.in.

various physical properties of these compounds. So in the present study, we have analysed the FS topology of the $LaRu_4X_{12}$ with X = P, As, Sb at ambient as well as under compression. Though there are a few reports available for $LaRu_4P_{12}$,[25] at ambient, high pressure studies are lacking for all the compounds which are presented quite elaborately in this work. The rest of the manuscript is organized as follows. The computational details regarding our calculations are presented in Sec. II; Sec. III includes the results and discussion of results pertaining to ambient pressure and under compression. Finally, Sec. IV concludes the paper.

II. METHOD OF CALCULATION

First-principles calculations were performed using the full-potential linearized augmented plane wave (FP-LAPW) method as implemented in the WIEN2k[26] code. For the exchange and correlation terms in the electron-electron interaction, we have used the generalized gradient approximation (GGA) of Perdew-Burke-Ernzerhof (PBE).[27] Muffin-tin radii are taken to be 2.5, 2.0, 1.75, 1.85, and 2.2 a.u for La, Ru, P, As, and Sb atom, respectively. A $30 \times 30 \times 30$ Monkhorst-Pack grid[28] of k-points has been used for the self-consistent field and density of states calculations. To ensure accurate determination of the Fermi level, we have used a $44 \times 44 \times 44$ k-point grid for Fermi surface calculation. The three-dimensional Fermi surface plots were generated with the help of the XCrySDen molecular structure visualisation program.[29] In order to achieve convergence of energy eigen values, the wave functions in the interstitial region were expanded using plane waves with $R_{MT}K_{max} = 10$ for X = As, Sb and $R_{MT}K_{max} = 9$ for X = P, where R_{MT} is the Muffin tin radius and the K_{max} gives the magnitude of the largest K vector in the plane-wave expansion. In the interstitial region, the charge density and the potential were expanded as a Fourier series with wave vectors up to $G_{max} = 9$, 12, 10 a.u.$^{-1}$ for X = P, As, Sb, respectively. The self-consistent calculations are considered to be converged when the total energy of the system is stable within 10^{-6} Ry. The calculations are carried out for the experimental lattice parameter. In the present study, the experimental volume of the system is represented by V_0. Experimental lattice parameters which we have used in our present calculation for $LaRu_4P_{12}$, $LaRu_4As_{12}$, and $LaRu_4Sb_{12}$ are 15.2333 a.u., 16.0812 a.u., and 17.5337 a.u., respectively. Calculations were performed with and without spin-orbit coupling (SOC) effect, and we have not noticed any pronounced SOC effect in the vicinity of the Fermi level and hence proceeded with our subsequent studies excluding the SOC effect. The de Haas van Alphen effect is calculated using the SKEAF programme.[30]

III. RESULTS AND DISCUSSION

A. Ground-state properties

The filled skutterudites of the form RT_4X_{12} have body centred cubic structure with space group $Im\bar{3}$ (204), where R is a rare-earth element, T is a transition metal element, and X is a pnictogen. The atomic position for R (R = La) is (0.0, 0.0, 0.0), T (T = Ru) occupies the position (0.25, 0.25, 0.25)

TABLE I. Calculated atomic position parameters u and v for $LaRu_4X_{12}$ with X = P, As, Sb.

Compounds		u	v
$LaRu_4P_{12}$	Present study	0.3577	0.1444
	Expt[a]	0.3591	0.1428
$LaRu_4As_{12}$	Present study	0.3501	0.1503
	Expt[a]	0.3500	0.1470
$LaRu_4Sb_{12}$	Present study	0.3418	0.1582
	Expt[a]	0.3400	0.1600

[a]Reference 31.

and X (X = P, As, Sb) is present at (0.0, u, v). We have relaxed the system to get the optimized values of (u, v) for all the investigated $LaRu_4X_{12}$ compounds. The experimental and calculated theoretical u and v positional parameters for X = P, As, Sb are tabulated in Table I. Our calculated values agree well with the experiment. The rest of the calculations are performed with the experimental lattice parameter along with the theoretical optimized atomic positions.

B. Band structure, density of states, and Fermi surface

The band structure for all the three compounds $LaRu_4X_{12}$ (X = P, As, Sb) is presented in Fig. 1 along the high symmetry directions without SOC because, as explained above, we find no significant change in the vicinity of the Fermi level by including SOC. Our calculated band structures agree well with the other available studies.[11,32] From the band structure plots, it is evident that, for $LaRu_4P_{12}$, three bands cross the Fermi level (E_F), whereas in the other two compounds, only two bands cross the E_F at ambient pressure. For all the three compounds, there is a relatively more dispersive conduction band (the band shown in black color in Fig. 1) which is of mixed orbital character at various points in the Brillouin zone. To further elucidate the nature of the bands, we have plotted *fat bands* for all the compounds in Fig. 2. It can be seen from the figure that the states in this conduction band are mainly of X-p_z character near the Gamma point, whereas the states near the N point are dominated by hybridized X-p_z, X-p_y and Ru-$d_{x^2-y^2}$, Ru-d_{xy} orbitals. While X-p_y, X-p_z together with admixture of the Ru-d_{z^2} character is dominant near the P point, the occupied states in this band near the H point have an admixture of the Ru-$d_{x^2-y^2}$, Ru-d_{xy}, Ru-d_{xz} and Ru-d_{yz} states. Apart from this, we have two more sets of bands for these compounds, one is the non-degenerate band (red color band as in Fig. 1) mainly derived from the Ru d_{z^2} at Γ point. We find this band to cross the E_F in the case of As and Sb containing compounds and possessing hole character, whereas it is below the E_F and completely filled in the case of $LaRu_4P_{12}$. The other set of doubly degenerate bands (blue and green color band in Fig. 1) is of X p_z (X = P, As, Sb) character and is again evident from Fig. 2. The same doubly degenerate band crosses the E_F only in the case of $LaRu_4P_{12}$ with hole character at the same Γ point, but in the case of As and Sb containing compounds, it is below the E_F and completely filled. In addition, to support our discussion, we have also calculated the l and m projected density of states as shown in
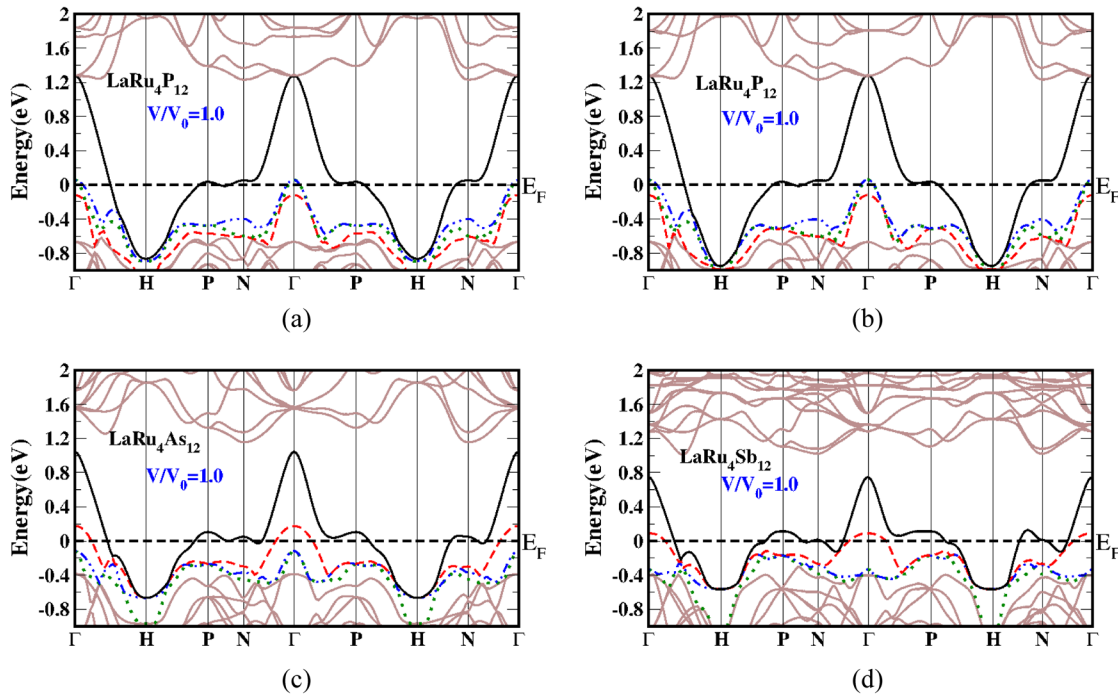
FIG. 1. Band structure of (a) $LaRu_4P_{12}$ with SOC and ((b)–(d)) for $LaRu_4X_{12}$ with X = P, As, Sb at $V/V_0 = 1.0$ without SOC. SOC effect in not seen in the vicinity of the Fermi level. The color code used for the plots is for identification of bands crossing the Fermi level. The high symmetry points Gamma, H, P, N correspond to (0, 0, 0), (0, 1, 0), (1/2, 1/2, 1/2) and (1/2, 1/2, 0) in the k-vector description with conventional basis. Equivalently, they correspond to (0, 0, 0), (0, 1/2, 0), (1/4, 1/4, 1/4) and (1/4, 1/4, 0) in the ITA (International Tables for Crystallography, Vol. A) description.

Fig. 3. Apart from this, we can see (Fig. 1) a pseudo gap above E_F in the band structure of As and Sb containing compounds, whereas the bands are found to be overlapping in the case of $LaRu_4P_{12}$ along the high symmetry direction studied in this work. This could be indicative of the presence of stronger bonding in As and Sb containing compounds in comparison with the P containing compound. To analyze this in detail, we have calculated the nearest-neighbour distance of the X-Ru and X-X atom pairs for all the three compounds. The nearest-neighbour distance between As-Ru and Sb-Ru is found to be 2.44 Å and 2.61 Å and is smaller than the calculated X-X distance of 2.55 and 2.93 Å for As and Sb, respectively. At the same time, the nearest-neighbour distance for P-Ru is 2.25 Å, which is larger than the P-P distance of 2.19 Å, indicating the interaction of P-Ru to be lesser in comparison with the P-P. On the other hand, we find the separation of the As(Sb)-Ru to be lesser leading to enhanced interaction between the atoms and ultimately creating a pseudo-gap above E_F,[33,34] which is well evident from the band structure plots in Fig. 1. Again our calculated fat bands shown in Fig. 2 depict the dominating nature of the Ru-d orbital at the vicinity of the Fermi level for As/Sb containing compounds than the P containing compound.

We have also analysed the contribution at the Fermi level from the different atoms through the partial density of states for these compounds as shown in Fig. 3. The density of states at the Fermi level is dominated by the Ru-d with admixture of the X-p (mainly p_y, p_z) orbitals. From the calculated total density of states, we find the highest peak at E_F in the case of $LaRu_4As_{12}$, followed by $LaRu_4Sb_{12}$ and $LaRu_4P_{12}$, with density of states at the Fermi level ($N(E_F)$) being 13.56, 11.16, 7.92 states/eV, respectively, which

alternatively give rise to the specific heat coefficient, γ, to be 31.96, 26.30, 18.67 mJ/mol K^2, respectively. Our calculated density of states for $LaRu_4P_{12}$ is in excellent agreement with the experimentally reported value of 7.14 states/eV (0.42 states/eV/atom).[12] We observe the computed total density of states as well as γ to be higher in $LaRu_4Sb_{12}$ as compared to $LaRu_4P_{12}$ which is suggestive of a larger electron-phonon coupling constant and hence a higher superconducting transition temperature T_c in the case of $LaRu_4Sb_{12}$ in comparison with $LaRu_4P_{12}$. However, the trend is reverse for the reported superconducting transition temperature. The experimentally reported values of T_c of $LaRu_4Sb_{12}$ is around 2.8 K[12] which is significantly lower in comparison with 7.2 K of $LaRu_4P_{12}$.[35]

To analyze in more detail the origin of the superconductivity, we have calculated the density of states at the Fermi level due to each band that crosses the E_F for all the compounds. From this analysis, we observe an unmistakable correlation between the calculated values of $N(E_F)$ corresponding to the more dispersive band (the black color band in Fig. 1) and the trend in the values of T_c of all the three compounds investigated here. The calculated value of $N(E_F)_{blackcolorband}$ is found to be 5.56, 8.91, and 7.26 states/eV for P, As, and Sb containing compounds, respectively, and seems to contribute nearly 65%–70% of the total $N(E_F)$. In the case of As and Sb containing compounds, the contribution due to the non-degenerate (red color) band (Fig. 1) may also play a role in the occurrence of superconductivity as we find the $N(E_F)$ due to this band to be 0.4 and 0.66 states/eV, respectively, and these two compounds might behave like a two band superconductor. On the other hand, the contribution from the doubly degenerate bands (blue and green band) is found to be only 0.08 and 0.03 states/eV, respectively, only in the case of
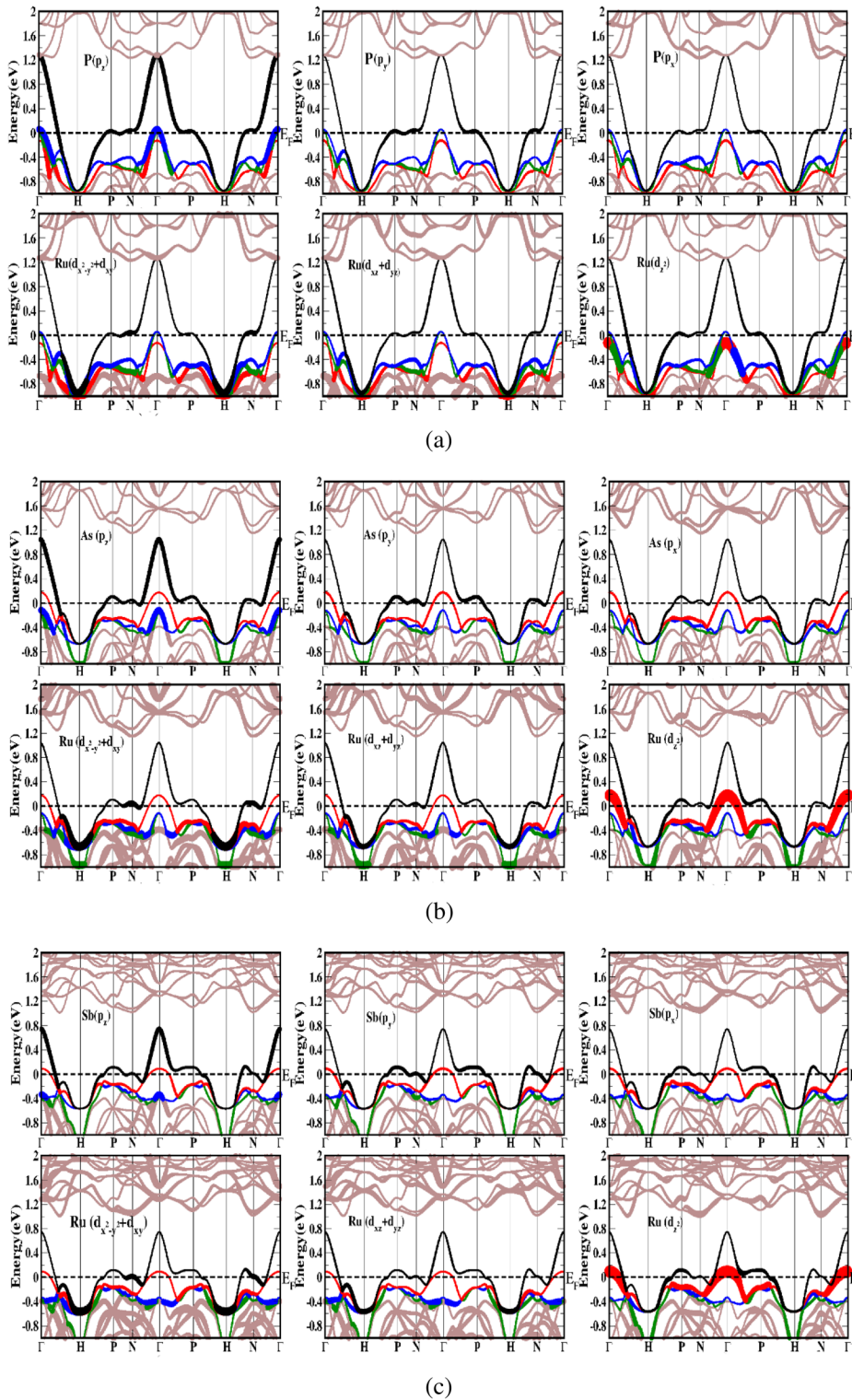
(a)

(b)

(c)

FIG. 2. Fat band of (a) LaRu$_4$P$_{12}$, (b) LaRu$_4$As$_{12}$, (c) LaRu$_4$Sb$_{12}$ at V/V$_0$ = 1.0. The color code used for the plots is for identification of bands crossing the Fermi level. The width of the band indicates the weight of each orbital contribution.

LaRu$_4$P$_{12}$ which is negligible in comparison with the black color band in this compound, and hence this compound might behave as a single band superconductor. At the same time, we also find the N(E$_F$) for the black color band in the case of LaRu$_4$As$_{12}$ to be highest, and the experimentally reported values of T$_c$ of this compound to be the highest.[12] This is in agreement with the conjecture that superconductivity arises primarily from this band, of hybridized X-p and Ru-d orbital character, in all these compounds. However, detailed *ab-initio* calculation of the electro-phonon coupling is necessary to validate this conjecture based on simple application of

McMillan's formula[36] with the assumption that λ is given by $N(E_F)\alpha$ and $\Theta_D = \beta/\sqrt{M}$, where α and β are assumed to be the same for all the three compounds that are studied, and M is taken to be the average mass per formula unit for each of the compounds.

Apart from this, we have studied the Fermi surface for all the compounds and find two hole pockets at Γ point in the case of LaRu$_4$P$_{12}$, as presented in Fig. 4 and are mainly of P-p_z orbital character. But only one hole pocket is visualised at Γ point for LaRu$_4$As$_{12}$ and LaRu$_4$Sb$_{12}$ and is mainly of Ru-d_{z^2} orbital character as discussed above. When we

(a)

(b)

(c)

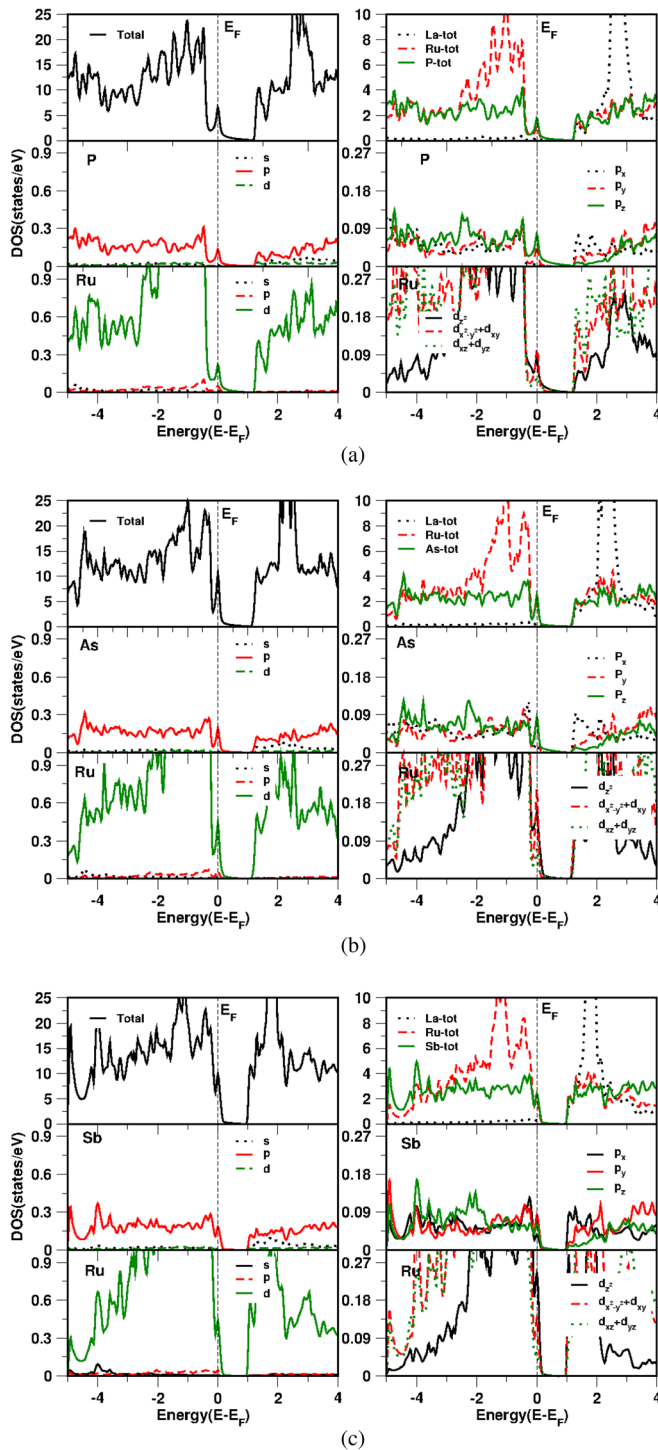FIG. 3. Total and partial density of states for LaRu4X12 with X = P, As, Sb at $V/V_0 = 1.0$. The different orbital contribution from different atoms is represented by various colors and symbols.

topology of this complicated surface is not the same for all the compounds due to the hybridisation of X-p (X = P, As, Sb) with Ru-d orbital and is confirmed from the fat bands presented earlier (Fig. 2). In the case of LaRu4P12, the complicated FS (Fig. 4(c)) consists of an open hole pocket around P-point in the FS and it connects to the remaining surface, resulting in the nesting property along PN direction with nesting vector q to be (1, 0, 0). The same nesting property is not expected in the case of LaRu4As12 and LaRu4Sb12, as we have not seen the same open hole sheet around P-point in the FS. Again the presence of the nearly flat band along PN direction in the case of LaRu4P12 support the observed nesting feature in P containing compounds. One more interesting feature in the complicated FS of these investigated compounds is the open orbit (especially at P and N points) FS in the case of LaRu4P12, which is completely different from the other compounds. In the case of LaRu4As12 and LaRu4Sb12, we find the FS sheet to be connected around P and N point just below the surface of the Brillouin zone, resulting in multiple opening in the sheet and is evident from Fig. 4. The dHvA study on LaRu4Sb12[19]
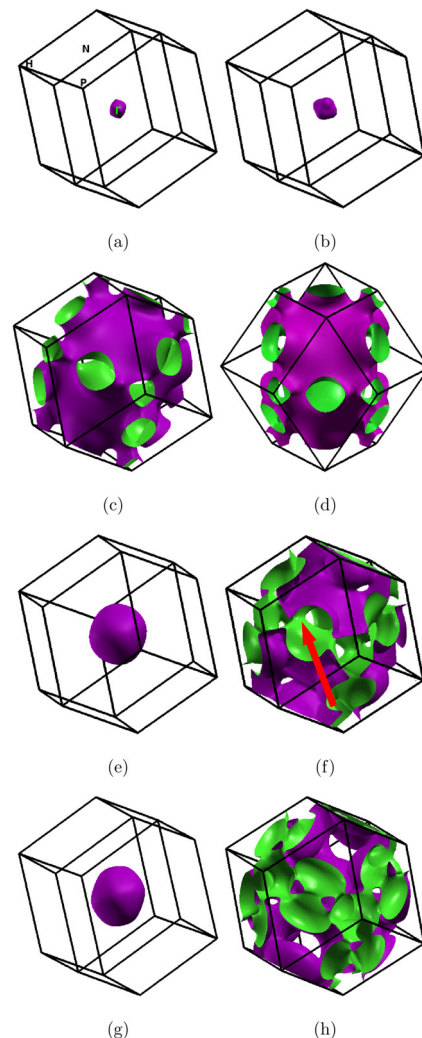
FIG. 4. Fermi surface of LaRu4X12 at $V/V_0 = 1.0$: (a)–(d) for LaRu4P12 with (c) and (d) corresponding to two different view points, (e) and (f) for LaRu4As12, (g) and (h) for LaRu4Sb12. (a), (b), (e), and (g) are hole pockets centered at Γ and (c), (d), (f), and (h) are the complicated FS derived from the black color band shown in Fig. 1.

compare the hole pockets of all the three compounds, we can see a completely spherical surface in the case of As and Sb containing compounds, which mainly derive from Ru-d_{z^2}. On the other hand, the hole surface of P containing compound is slightly elongated and is derived from the P-p_z orbital. Our calculated Fermi surfaces compare well with the previous study.[11] In addition to this, we have a complicated FS sheet due to the other band (see solid black color band in Fig. 1), which is more dispersive and crosses the E_F at several high symmetry points for all the compounds. But the

FIG. 5. Band structure of LaRu$_4$X$_{12}$ with X = P, As, Sb at V/V$_0$ = 0.8. Color code used for the plots is similar at ambient and compressed volumes to identify the changes in band structure under compression.

show three branches and the authors further expect two branches to originate from the multiply connected FS, which agree well with our calculation as shown in Fig. 4(h).

C. Effect under compression

Under compression, we observe an opposite movement of the non-degenerate and doubly degenerate bands irrespective of their position at the Γ point, and the band structure under compression at V/V$_0$ = 0.8 is shown in Fig. 5. The non-degenerate band (mainly derived from the Ru-d_{z^2} orbital) shifts down and the degenerate bands (mainly derived from the X-p_z orbital) shift up under compression. In other words, we can say that the non-degenerate band gets populated and

the doubly degenerated bands get depopulated under compression, resulting in the electron concentration of the Ru-d_{z^2} orbital to increase and the corresponding electron concentration in the X-p_z orbital decreases. Due to this, in LaRu$_4$P$_{12}$, the size of the two hole pockets increases under compression but the topology remains the same as evident from the band structure plots in Fig. 5, and in the other two compounds, the hole pockets get reduced in size and finally at V/V$_0$ = 0.80, the hole pocket vanishes only in the case of LaRu$_4$Sb$_{12}$. In addition in the complicated sheet, the opening along *PN* direction in the case of the Sb containing compounds get reduced. In the case of LaRu$_4$As$_{12}$, under compression, we observe two extra hole pockets at Γ point (Fig. 6) due to the upward movement of the doubly degenerate bands but not in
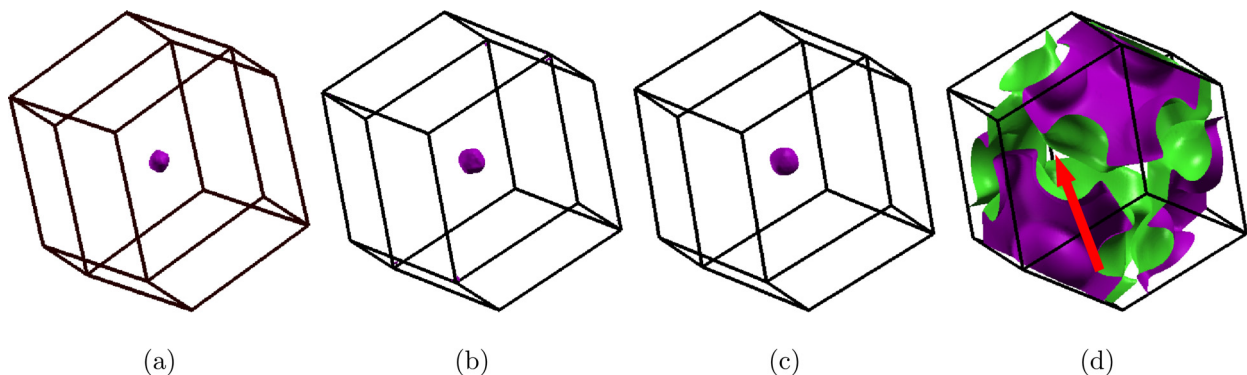

FIG. 6. Fermi surface of LaRu$_4$As$_{12}$ at V/V$_0$ = 0.8. (a) and (b) are the two new hole pockets that appeared under compression. The arrow mark indicates the observed change at V/V$_0$ = 0.8 with respect to V/V$_0$ = 1.0 (Fig. 4(e)).

the case of $LaRu_4Sb_{12}$ due to the positioning of the band more deeper in energy and is well evident from Figs. 1(d) and 5(c). The main interesting feature in $LaRu_4As_{12}$ is the FS topology change under compression in the complicated surface, where we find the interconnected sheets to separate and the FS contains multiple sheets centered at H point in the Brillouin zone and is well evident from arrow mark in the FS figure in Figs. 4(e) and 6(d). So the appearance of new pocket may render $LaRu_4As_{12}$ a multiband super-conductor under compression. But the topology of the complex surface of $LaRu_4P_{12}$ remains unchanged under compression.

Apart from this, we find the $N(E_F)$ due to the black color band to decrease for all the investigated compounds under compression, but the rate of decrease is less in P and Sb containing compounds in comparison to the As containing compound, and the values are 3.74, 4.7 and 5.4 states/eV for P, As, Sb containing compounds, respectively. This observed drastic decrease in $N(E_F)$ in the case of $LaRu_4As_{12}$ may cause reduction in T_c under compression, and the superconducting transition temperature might be in the same range as of the P and Sb containing compounds. This observed change in the case of As containing compound among these investigated compounds may be due to the observed FS topology change in the complicated sheet, which is mainly derived from the black color band.

Apart from this, we have calculated the dHvA frequency for all the compounds at ambient as well as under compression, and the character of the dHvA orbits is tabulated in Table II. In all, our study revealed a number of frequency branches for the complicated Fermi surface of the compounds studied, and some of the branches are also having multiple copies of orbits at ambient pressure as well as under compression. The dHvA frequency is found to be higher in $LaRu_4As_{12}$ than $LaRu_4Sb_{12}$ for the first band, which is derived from the Ru-d_z^2 orbital in both the compounds. More interestingly, we observe the number of dHvA frequency branches to be reduced in the As and Sb containing compounds under compression, where we have also found the Fermi surface topology to change. But the number of extremal orbits is found to be same for $LaRu_4P_{12}$ under compression, and we also have not found any Fermi surface topology change till higher compression and is clearly evident from our calculated values as reported in Table II. In the case of $LaRu_4As_{12}$, we have nine different branches at ambient pressure with different frequencies and the values are reported in Table II. At compression $V/V_0 = 0.8$, we have seen all the orbits to disappear for this compound except two orbits positioned at (0.5 0.5 0.5) and (0.51 0.48 0.46) which are having frequencies 7.03 and 7.19 kT, respectively, at ambient. Similarly in the case of $LaRu_4Sb_{12}$, we have seen few branches to disappear and a few new branches to appear under compression at $V/V_0 = 0.8$. We find the branches with frequencies 0.496, 0.596, 1.12, 1.2, 1.397, 1.399, 5.357, 5.4, and 5.69 kT at ambient pressure to disappear under compression and simultaneously the branches with frequencies 0.0138, 1.40, 3.84, and 5.24 kT are found to appear at $V/V_0 = 0.8$ and well support the FS topology change. Overall the number of frequency branches is found to be

TABLE II. dHvA orbits for $LaRu_4X_{12}$ with X = P, As, Sb. The symbols "e" and "h" represent the electron and hole character of the orbit. Frequency F is given in kilo Tesla.

Band number	V/V_0	F (kT)	m^* (m)	Number of orbits	Type
$LaRu_4P_{12}$					
1	1.0	0.119	0.229	1	h
	0.8	0.61	0.27	1	h
2	1.0	0.2	0.401	1	h
	0.8	0.86	0.395	1	h
3	1.0	0.163	1.668	2	e
		0.59	1.42	1	h
		1.29	5.15	2	h
		6.5	4.95	2	h
	0.8	0.134	1.288	2	e
		0.64	1.12	1	h
		0.135	1.29	2	e
		1.55	3.67	2	h
$LaRu_4As_{12}$					
1	1.0	1.15	0.756	1	h
	0.8	0.145	0.478	1	h
2	1.0	0.0387	1.2	2	e
		0.0394	1.18	2	e
		0.043	1.31	2	e
		0.044	1.27	2	e
		0.692	1.41	1	h
		0.693	1.43	1	h
		6.84	5.06	2	e
		7.03	4.32	1	e
		7.19	5.26	2	e
	0.8	8.16	3.59	1	e
		8.17	3.76	1	e
3	0.8	0.078	0.206	1	h
4	0.8	0.117	0.454	1	h
$LaRu_4Sb_{12}$					
1	1.0	0.952	0.993	1	h
	0.8	…	…	…	…
2	1.0	0.057	0.55	2	e
		0.0825	0.738	1	h
		0.0842	0.742	1	h
		0.273	0.796	2	e
		0.496	0.54	4	h
		0.596	1.1	2	e
		1.013	1.13	2	h
		1.12	2.15	4	h
		1.2	1.3	1	e
		1.2	1.2	1	e
		1.397	2.93	2	h
		1.39	2.94	2	h
		5.24	4.01	1	h
		5.35	4.98	1	e
		5.356	5.33	1	e
		5.357	4.78	1	e
		5.4	5.04	2	e
		5.69	3.85	2	e
	0.8	0.0136	0.367	2	e
		0.0138	0.368	2	e
		0.233	0.696	2	e
		0.268	1.02	1	h
		0.272	1.03	1	h
		0.627	1.44	2	e
		1.40	1.51	1	e
		1.43	9.16	2	h

TABLE II. (*Continued.*)

Band number	V/V$_0$	F (kT)	m* (m)	Number of orbits	Type
		3.84	4.85	2	h
		5.24	5.6	2	h
		6.19	3.69	1	e
		6.20	3.62	1	e
		6.21	3.88	1	e
		6.34	3.79	1	e

decreased under compression in the case of As and Sb containing compounds.

IV. CONCLUSION

The band structure, density of states, and Fermi surface have been investigated for the filled skutterudites compounds LaRu$_4$X$_{12}$ with X = P, As, Sb. The states at the Fermi level are found to be dominated by the Ru-d with the admixture of X-p orbitals. We find three FS for the P containing compounds and two FS for the As and Sb containing compounds. Among these surfaces, the hole pocket centered at Γ is mainly derived from the P-p_z orbital in the case of LaRu$_4$P$_{12}$, and the same hole surface for LaRu$_4$As$_{12}$ and LaRu$_4$Sb$_{12}$ is found to be mainly from the Ru-d_{z^2}. Among all these three compounds, the nesting feature is expected only in LaRu$_4$P$_{12}$ and a drastic Fermi surface topology change is observed in the complicated sheet under compression in LaRu$_4$As$_{12}$. From the FS change, we predict LaRu$_4$As$_{12}$ to be a multi band superconductor. In addition, from the dHvA calculation, we find the number of extremal orbits to vary for the complicated FS sheet in the case of As and Sb containing compounds under compression, where we have also seen the FS topology to change, whereas no such change is observed for P containing compound at ambient pressure as well as under compression.

[1]A. Miyake, K. Shimizu, C. Sekine, K. Kihou, and I. Shirotani, J. Phys. Soc. Jpn. **73**, 2370 (2004).
[2]K. Hachitani, H. Fukazawa, and Y. Kohori, Phys. Rev. B **73**, 052408 (2006).
[3]H. Sato, H. Sugawara, D. Kikuchi, S. Sanada, K. Tanaka, H. Aoki, K. Kuwahara, Y. Aoki, and M. Kohgi, Physica B **378–380**, 46 (2006).
[4]H. Sugawara, T. D. Matsuda, K. Abe, Y. Aoki, H. Sato, S. Nojiri, Y. Inada, R. Settai, and Y. Ōnuki, Phys. Rev. B **66**, 134411 (2002).
[5]E. D. Bauer, N. A. Frederick, P.-C. Ho, V. S. Zapf, and M. B. Maple, Phys. Rev. B **65**, 100506(R) (2002).
[6]Y. Aoki, A. Tsuchiya, T. Kanayama, S. R. Saha, H. Sugawara, H. Sato, W. Higemoto, A. Koda, K. Ohishi, K. Nishiyama, and R. Kadono, Phys. Rev. Lett. **91**, 067003 (2003).
[7]H. Harima and K. Takegahara, J. Phys.: Condens. Matter **15**, S2081 (2003).
[8]G. S. Nolas, D. T. Morelli, and T. M. Tritt, Annu. Rev. Mater. Sci. **29**, 89 (1999).
[9]G. J. Snyder and E. S. Toberer, Nature Mater. **7**, 105 (2008).
[10]B. C. Sales, D. Mandrus, and R. K. Williams, Science **272**, 1325 (1996).
[11]S. R. Saha, H. Sugawara, Y. Aoki, H. Sato, Y. Inada, H. Shishido, R. Settai, Y. Ōnuki, and H. Harima, Phys. Rev. B **71**, 132502 (2005).
[12]T. Uchiumi, I. Shirotani, C. Sekine, S. Todo, T. Yagi, Y. Nakazawa, and K. Kanoda, J. Phys. Chem. Solids **60**, 689 (1999).
[13]M. M. Koza, D. Adroja, N. Takeda, Z. Henkie, and T. Cichorek, J. Phys. Soc. Jpn. **82**, 114607 (2013).
[14]Y. Kawamura, T. Kawaai, J. Hayashi, C. Sekine, H. Gotou, J. Cheng, K. Matsubayashi, and Y. Uwatoko, J. Phys. Soc. Jpn. **82**, 114702 (2013).
[15]H. Harima and K. Takegahara, Physica C **388–389**, 555 (2003).
[16]H. Harima and K. Takegahara, Physica B **403**, 906 (2008).
[17]H. Sugawara, Y. Abe, Y. Aoki, H. Sato, M. Hedo, R. Settai, Y. Ōnuki, and H. Harima, J. Phys. Soc. Jpn. **69**, 2938 (2000).
[18]S. R. Saha, H. Sugawara, R. Sakai, Y. Aoki, H. Sato, Y. Inada, H. Shishido, R. Settai, Y. Ōnuki, and H. Harima, Physica B **328**, 68 (2003).
[19]H. Sugawara, K. Abe, T. D. Matsuda, Y. Aoki, H. Sato, R. Settai, and Y. Ōnuki, Physica B **312–313**, 264 (2002).
[20]L. Bochenek, R. Wawryk, Z. Henkie, and T. Cichorek, Phys. Rev. B **86**, 060511(R) (2012).
[21]T. Namiki, Y. Aoki, H. Sato, C. Sekine, I. Shirotani, T. D. Matsuda, Y. Haga, and T. Yagi, J. Phys. Soc. Jpn. **76**, 093704 (2007).
[22]R. W. Hill, L. Shiyan, M. B. Maple, and L. Taillefer, Phys. Rev. Lett. **101**, 237005 (2008).
[23]K. Koga, K. Akai, K. Oshiro, and M. Matsuura, Phys. Rev. B **71**, 155119 (2005).
[24]I. Shirotani, T. Uchiumi, K. Ohno, C. Sekine, Y. Nakazawa, K. Kanoda, S. Todo, and T. Yagi, Phys. Rev. B **56**, 7866 (1997).
[25]K. Takegahara and H. Harima, J. Magn. Magn. Mater. **310**, 861 (2007).
[26]P. Blaha, K. Schwarz, G. K. H. Madsen, D. Kvasnicka, and J. Luitz, *WIEN2K, An Augmented Plane Wave + Local Orbitals Program for Calculating Crystal Properties* (Karlheinz Schwarz, Techn. Universität Wien, Austria, 2001).
[27]J. P. Perdew, K. Burke, and M. Ernzerhof, Phys. Rev. Lett. **77**, 3865 (1996).
[28]H. J. Monkhorst and J. D. Pack, Phys. Rev. B **13**, 5188 (1976).
[29]A. Kokalj, Comput. Mater. Sci. **28**, 155 (2003).
[30]P. M. C. Rourke and S. R. Julian, Comput. Phys. Commun. **183**, 324 (2012).
[31]I. Shirotani, private communication.
[32]J. Yang, R. Liu, Z. Chen, L. Xi, J. Yang, W. Zhang, and L. Chen, Appl. Phys. lett. **101**, 022101 (2012).
[33]A. Pasturel, C. Colinet, and P. Hicter, Physica B+C **132**, 177–180 (1985).
[34]C. D. Gelatt, Jr., A. R. Williams, and V. L. Moruzzi, Phys. Rev. B **27**, 2005–2013 (1983).
[35]J. Hayashi, K. Akahira, K. Matsui, H. Ando, Y. Sugiuchi, K. Takeda, C. Sekine, I. Shirotani, and T. Yagi, J. Phys.: Conf. Series **215**, 012142 (2010).
[36]W. L. McMillan, Phys. Rev. **167**, 331–344 (1968).